

ANALYSIS OF DRYING SHRINKAGE'S SURFACE CRACKING IN CONCRETE BY BEAM-PARTICLE APPROACH

N. CHAN*, C. OLIVER-LEBLOND*, F. BENBOUDJEMA* AND F. RAGUENEAU*

*LMT, ENS Cachan
CNRS, Université Paris-Saclay
94235 Cachan, FRANCE
e-mail: nchan@lmt.ens-cachan.fr

Key words: Beam-particle approach, Drying shrinkage, cracking, virtual testing, Durability

Abstract. In this paper, investigations are focused on the beam-particle model to analyze the impact of drying shrinkage cracking. The cohesion of particles is achieved with an Euler-Bernoulli lattice brittle beams. In case of cracking, cohesion disappears and the contact law with friction is considered between the polygonal particles. In the model, the shrinkage's strain field is obtained by from classical continuous method resolution. Beam-particle model permits to obtain local cracking patterns from finite element drying strain results. In order to model shrinkage and local crack, hydric and mechanical weak coupling is investigated with discrete approach. It demonstrates that the material's history influences the structural response. Moreover, shrinkage cracks are visualized on experimental specimens' surfaces. In order to quantify the size of the crack's surface an apparent radius is calculated to obtain a statistical repartition. Numerically, surfaces cracking tests were analyzed to model responses with different boundary conditions The data reveals that cracks propagation is deeply correlated with the hydric gradient on the borders of the specimen.

1 INTRODUCTION

Concrete constructions have been designed for a certain service life. Cement-based materials are commonly used in construction due to the abundance of basic minerals on earth. They are undergoing shrinkage and especially drying shrinkage. It is essential to predict their durability to ensure a safe structure, during all the lifespan. Indeed, due to moisture difference between the material's core and the external environment, a hydric moisture gradient locally induces tensile and compressive stresses, that may lead to cracks. These phenomena are also amplified with external restraints : wall/slab; rendering mortar, concrete lift, etc. Cracks and especially micro-cracking network have a direct impact on transfert property : permeability, diffusivity and mechanical behavior. It is a cat-

alyzer for concretes durability issue : carbonation, chloride attack, swelling which impacts both mechanical and hydric properties. Therefore, it is necessary to consider drying shrinkage to study cementitious materials cracking and behavior. Numerically, it is scarce to consider the material's history in a structure calculus. In this work, the impact of drying shrinkage is analyzed before a three points bending test. Beam-particle approach is implemented to explicitly describes drying and mechanical cracks. Spatial discretization is based on particles of Voronoï tessellation. The dual Delaunay triangularisation represents material's cohesion which is obtained with a lattice Euler-Bernoulli brittle beams. In order to reproduce cracks closure and unilateral effect [3], polygonale particles interact with friction contact law due to

fragile behavior in mechanical tests [1] [10] . The hydric phenomena are modelled with a finite element approach. Information of Gauss strains points are projected on lattice discretization. Then, the beam-particle approach and the damage model are compared.

In this article, a beam behavior is investigated, the rugosity of crack pattern will be presented in the next work, that's why only 2D numerical experiments are necessary and investigated.

2 DRYING SHRINKAGE

Drying shrinkage occurs during the whole life of cimentious materials. Formed crack catalyze the concrete's damage and reduce its lifespan. To model this phenomenon, differential equation of classical diffusion (1) permits to represent the gradient of humidity between intern and external moisture.

$$\phi \frac{\partial S}{\partial P_c} \frac{\partial P_c}{\partial t} = \left(\frac{K k_r}{\mu} \text{grad}(P_c) \right) \quad (1)$$

In this equation ϕ represents porosity, S the degree of saturation, P_c capillar pressure, k_r relative permeability, K permeability, μ water viscosity. To represent the hydric gradient near the material surface, the model needs the external moiture experimentally measured and the internal moisture which is supposed almost equal to 100% due to the high water/ciment ratio (2). Non linear terms are expressed in saturation and pressure gradient.

$$P_c = \frac{\rho R T}{M} \ln(HR) \quad (2)$$

Capillary suction explains the cohesion of granular material. Van Genuchten model [9] for desorption isotherm permit to calculate the saturation of material (3), with two parameters a and m .

$$S(P_c) = \left(1 + \left(\frac{|P_c|}{a} \right)^{\frac{1}{1-m}} \right)^{-m} \quad (3)$$

$$k_r = \sqrt{S} \left(1 - \left(1 - S^{\frac{1}{m}} \right)^m \right)^2 \quad (4)$$

Relative permeability is estimated with the same model (4)

Concerning the porosity, it is experimentally estimated with a drying test [8]. Concrete specimen is heated step by step to $60^\circ C$ until mass stabilisation. Drying shrinkage strain and relative humidity are correlated by a linear relation.

Note that, drying and drying shrinkage simulations are performed by finite element model.

3 BEAM-PARTICLE APPROACH

Based on solid mechanics, beam-particle approach meshing consists on Voronoï tessellation and Delaunay triangulation duality. On figure 1 Voronoï tessellation represents material discretization. Delaunay triangulation is the material's cohesion.

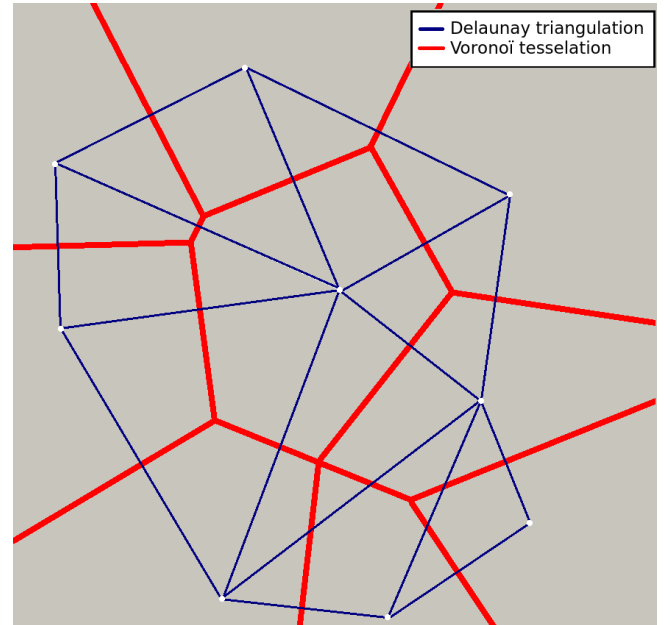


Figure 1: Space discretization and cells cohesion

The advantage of this method is the fact that it is simple and fastly generated compared to a mesh composed of disk. The spatial discretization is constituted of polygonal cells, figure 2, which are characterized by a unique seed, generated randomly.

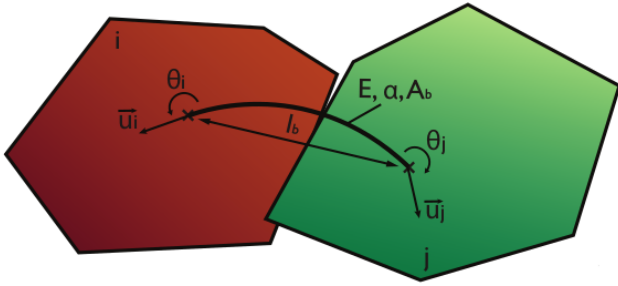


Figure 2: Two particles linked [10]

Each cell has three degrees of freedom, two in translation \vec{U}_x, \vec{U}_y , and one in rotation $\vec{\theta}$. Then, the cohesion of the material is defined by a brittle Euler-bernoulli lattice which is connected to each seed. Lattice beams are characterized respectively by E, α, A_b, l_b , the young modulus, the inertia, the cross section and the length. Brittle beam is driven by a failure criteria, considering beam strain and rotation, figure 3.

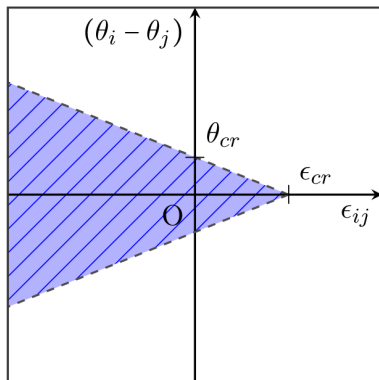


Figure 3: Lattice failure criterion [10]

The particle’s interaction is defined by the Coulomb friction law in order to represent crack closure and energy dissipation.

As presented before, the drying shrinkage is realized with a classical continuous approach. Then, the strain field on Gauss point is projected and interpolated on each seed of cell. Beam-particle method has to reequilibrate intern and external force. The beam’s failure criterion generates local cracks.

4 VIRTUAL TESTING

In this part, a limit of finite element representation is highlighted. Then, classical isostatic three points bending flexural tests are investigated with the beam-particle approach. The influence of drying shrinkage on the mechanical behavior is analyzed.

Numerical parameters are identified on an experimental campaign [8]. The considered beam is EDF Vercors formulation [11]. It is a $84 \times 10 \times 10 \text{ cm}$ dimensions concrete conserved in a temperature and moisture control room, respectively 20°C and 30% HR.

Concerning spatial discretization, a preliminary analysis is realized to obtain an isotropic orientation of each lattice. Cracks pattern description is directly correlated with polygons size. Then, Young’s modulus and Poisson ratio are also identified with experimental measures.

In this study, Voronoï’s cells are in average 2 cm wide and high. Discretization implicates 60000 degrees of freedom.

4.1 Impact of drying shrinkage

During the drying shrinkage, an hydric gradient appears due to the difference of moisture in the material and the environnement. It locally creates, compressive constraint in the center of the specimen, and tensile constraint at the border. Shrinkage cracks occur because of the weak tensile resistance.

Drying shrinkage model is based on capillarity pressure resolution. Experimental boundary conditions are applied. In the numerical model, saturation is calculated for each timestep. Then, a linear model permits to determined the equivalent strain field. Mazars’ model is used to represent damage.

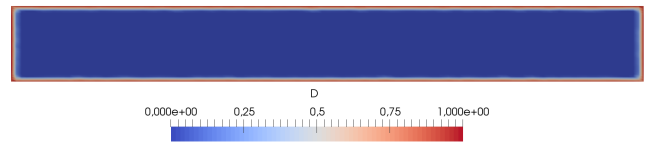


Figure 4: Numerical drying shrinkage damage

On figure 4, shrinkage drying damage is rep-

resented. Concrete borders are totally damaged and non localized. Finite element does not correctly consider shrinkage cracking pattern due to Galerkin’s continuum formulation. Experimentally, cracks are localised on the surface and on borders, figure 5. It is possible to characterize the surface cracking area’s surface of macroscopic cracks with a numerical approach.

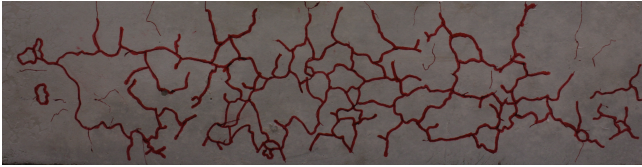


Figure 5: Experimental drying surface cracking

The picture 6 is an example of surface cracking. It is transformed in a black and white image. Then, some filter are used and the skeleton of crack pattern is kept. A pixel represents $50\mu m$. In order to estimate the area of surface cracking, erosion and dilation methods are developed [2]. These tools permit to locally rearrange pixel so as to generate a continuous line. In figure 5 some surface cracking are closed.

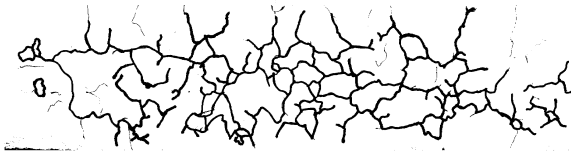


Figure 6: Binary image

The size of each closed surface, an equivalent radius, the area-surface ratio, is estimated, figure 7, on several concrete surfaces. The distribution of the equivalent radius seems to describe a Weibull repartition.

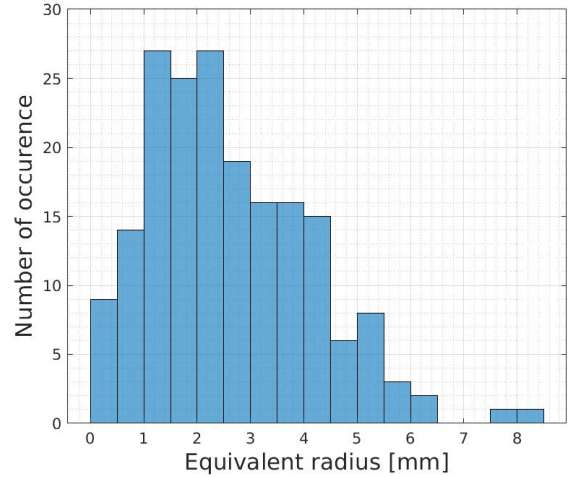


Figure 7: Distribution of equivalent radius

Several methods are proposed in literature to describe discontinuity: Enrich finite element, such as, X-FEM [4], E-FEM [6]. This study focuses on discrete element method, especially beam-particle approach.

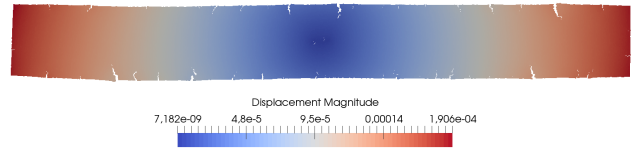


Figure 8: Drying shrinkage cracking pattern (x400)

In order to obtain more realistic cracking patterns, finite element shrinkage strain field is projected on a beam-particle discretization [5]. Each Gauss point is interpolated on a discrete element. Shrinkage strain field is decoupled from mechanical part and acts as an external force (5). Crack occurs for each lattice which reaches the failure criterion. It is justified to decouple drying shrinkage and three points bending test. Indeed mechanical testing time is significantly shorter than hydric effect.

$$\mathbf{K}\mathbf{u} = \mathbf{f}_{\text{ext}} + \mathbf{f}_{\text{sh}} \quad (5)$$

With \mathbf{K} , the stiffness matrix, \mathbf{u} the displacement vector, \mathbf{f}_{ext} the external force, \mathbf{f}_{sh} the equivalent shrinkage loading.

One advantage of discrete element is the natural cracking pattern representation because it

is based on solid mechanics. Cracks are obtained only with mechanical equilibrium. In this model, only macroscopic cracks are represented.

4.2 Mechanical behavior

In this part, the mechanical behavior of the beam figure 9 is tested on a three point bending setup. Several characteristics are considered : drying shrinkage and notch. For each case, the force-displacement curve is presented and discussed.

Due to the random characteristics, the presented curves are a mean value of several numerical three points bending tests.

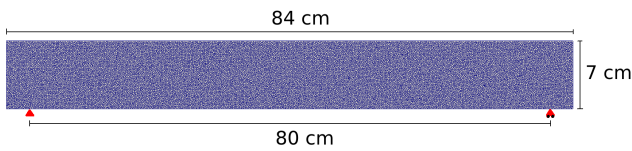


Figure 9: Concrete beam

4.2.1 Three points bending without drying

This first case considers that the material is not submitted to drying shrinkage. Experimentally, the beam is conserved in endogenous conditions in water or in a high humidity room. Theoretically, the beam cannot shrink because moisture between the material and the environment are already in an equilibrium state. However, additional phenomena such as autogenous shrinkage or carbonation are not considered in the numerical model. They are neglected, compared to drying shrinkage.

In figure 10, the quasi-brittle material has maximum flexural strength of 4.1 kN for 0.16 mm of displacement. This case permits to identify numerical parameters and calibrate them to experimental datas : lattice cohesion property, cells rotation or friction between cells.

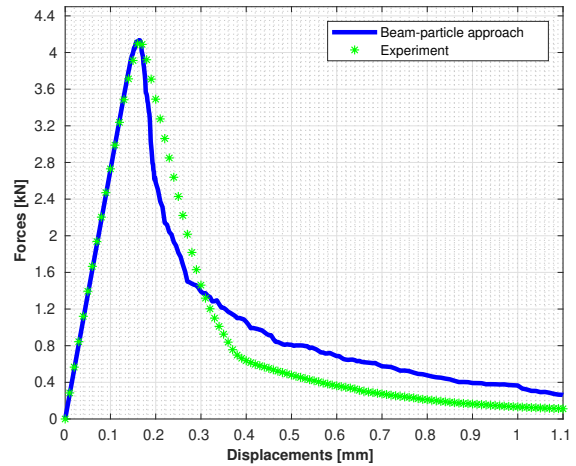


Figure 10: Only three points bending test

4.2.2 Three points bending with drying

In this case drying shrinkage is modeled with finite element and projected on beam particle discretization, as explained before. Then the last drying displacement field constitutes the initial state in the mechanical experiment. Cracks are generated due to high moisture gradient at the surface of concrete. Shrinkage drying cracking is also considered and supposed homogenous. Cracks occurring do not depend on geometry, in this case.

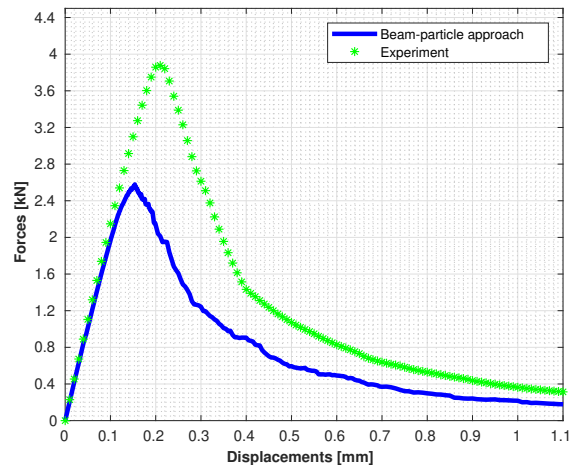


Figure 11: Drying shrinkage + 3 points bending

For flexural test, the upper fiber of the beam is under compression. Contact and friction law

control cracks closure. the low fiber is in a tensile state.

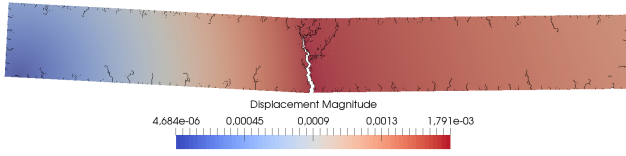


Figure 12: Cracking pattern (x8)

Compared to the first case, maximal flexural strength collapses to 40%, figure 11. However, this result is in accordance with finite element resolution because both results predict almost the same behavior. The reason of a decrease of the maximal strength is different for continuous and discontinuous approach. Indeed, for finite element the strength reduction is due to the healthy section. Maximum damage is considered which does not reflect reality. As demonstrated in figure 4, the diffuse damage reduces the section of interest. For beam-particle, the reduction is provoked by initial cracks. Indeed, a mechanical main crack is initiated on a drying shrinkage cracks. So, this crack can seem to be a notch. In certain cases, drying has no impact on mechanical properties for that reason. However, in three points bending, cracking is forced in the middle of the beam due to the local maximal moment. A correlation can be done on the quantity of cracks and the mechanical behavior.

4.2.3 Notched three points bending

The same numerical test is realized on notched beam to analyze the influence of mechanical property.

The notch is realized just before the mechanical test. Notched and unnotched beam are modelled without adding new parameters.

Figure 13 presents the result of notched-unnotched identification, according to RILEM experimental recommendation [7]. The notch is 2mm wide and correspond to the mean size of cells. Compared to the first case, flexure maximal strength decrease. Cracks is localized and the mechanical behavior is less brittle.

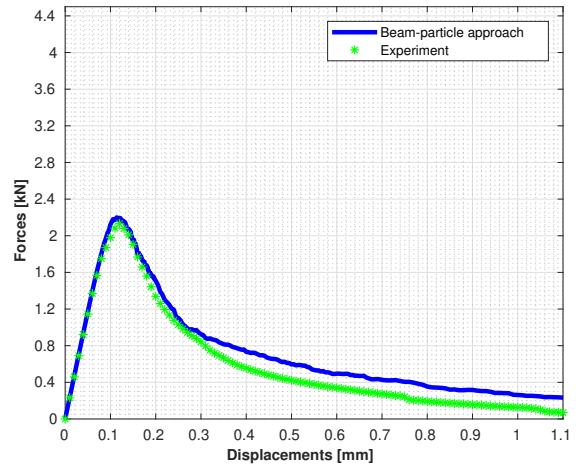


Figure 13: Notched three points bending

4.2.4 Notched three points bending with drying

The curve, figure 14 represents the prediction of drying shrinkage on a notched beam. The maximal flexural strength does not have a significant difference, compared to figure 13. This observation indicates that in the model, drying shrinkage has no impact on mechanical behavior.

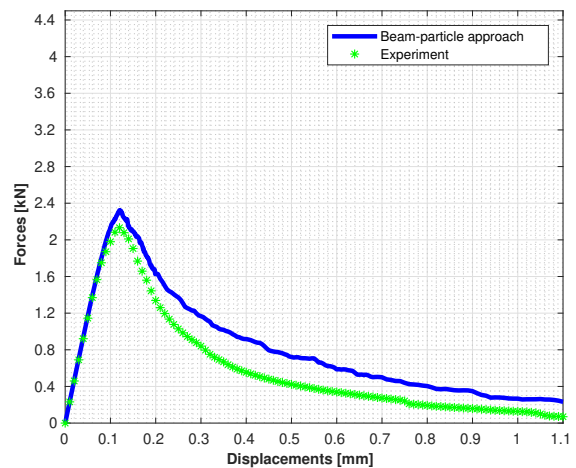


Figure 14: Drying shrinkage + bending

This result is logical because the notch is created after the drying. So, drying shrinkage cracks cannot occur in the notch area. Experi-

mentally, micro-cracks are induced by the cutting action.

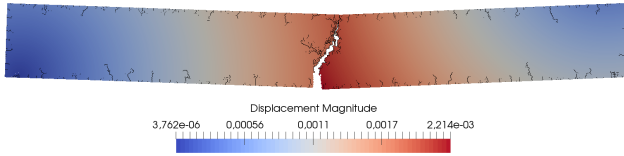


Figure 15: Notched cracking pattern (x8)

The difference between figure 14 and figure 13 comes from the initial displacement field. It also demonstrates that cracks localisation initiation, limitate drying shrinkage effect.

5 CONCLUSION

In this study, the influence of drying shrinkage is analyzed. It reveals that mechanical behavior is directly impacted by drying shrinkage. The result indicates that the prediction is underestimated because of maximal strength peak loss, with continuous and discontinuous approach. However, creep and capilarity suction relax constraint in order to increase the maximal flexure strength peak [8]. In beam-particle-approach, the mechanical behavior is directly correlated with cracks position and mechanical cracks initiation.

REFERENCES

- [1] D' Addetta., G. A., 2004. *Discrete models for cohesive frictional materials, Ph.D. thesis, Universitt Stuttgart.*
- [2] Hosseini M., 2015. *Numerical simulation of hydro-mechanical behavior of nanoporous materials: application to cement paste, university Lille 1*
- [3] Mazars, J. B. 1990. *The unilateral. Eng. Fract. Mech.*, 35 :629 - 635.
- [4] Moes, N. D. 1999. *A finite element method for crack growth without remeshing. international journal for numerical methods. Engineering*, 46(1) :131 - 150.
- [5] Oliver-Leblond. Cécile, 2013. *Two scale description of local mechanisms : application to reinforced concrete, Ecole normale supérieure de Cachan - ENS Cachan*
- [6] Ortiz, M. L. 1987. *A finite element method for localized failure analysis. computer methods in applied mechanics and engineering. Engineering*, 61(2) :189 - 214.
- [7] Rilem, 1985. *Determination of the fracture energy of mortar and concrete by means of three-point bend tests on notched beams, V01. 18 - N 106 - Matériaux et Constructions* 287 - 290
- [8] Soleilhet,F., 2018. *Experimental and numerical investigations of cementitious materials under hydro-mechanical loadings, Université Paris-Saclay*
- [9] Van Genuchten, M. (1980). *A closed-form equation for predicting the hydraulic conductivity of unsaturated soils. Soil Science of America Journal*, 44:892 - 898.
- [10] Vassaux,M., Ragueneau,F., Richard,B., Millard,A., 2014. *Compressive behavior of a lattice discrete element model for quasi-brittle materials, Computational Modelling of Concrete Structures* 335 - 344.
- [11] VeRcoRs, 2017. *de FRANCE , E. Site web projet vercors.*